

# Lawrence Berkeley National Laboratory

## Recent Work

### Title

QUANTITATIVE ASPECTS OF DEUTERON (SPIN 1) SPIN-DECOUPLING IN SOLIDS

### Permalink

<https://escholarship.org/uc/item/7tx2j5w3>

### Author

Suwelack, D.

### Publication Date

1978

Submitted to Chemical Physics

UC-34C  
LBL-7373 c.1  
Preprint

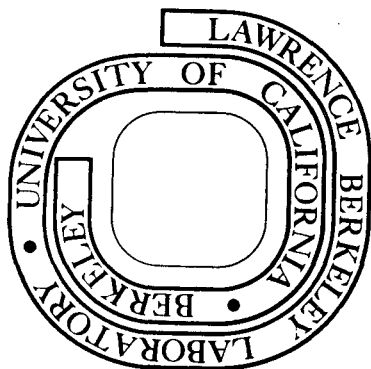
QUANTITATIVE ASPECTS OF DEUTERON  
(SPIN 1) SPIN-DECOUPLING IN SOLIDS

D. Suwelack, M. Mehring, and  
A. Pines

January 1978

Prepared for the U. S. Department of Energy  
under Contract W-7405-ENG-48

**For Reference**  
Not to be taken from this room



RECEIVED  
JAN 29 1979  
LIBRARY AND DOCUMENTS SECTION

LBL-7373  
c.1

## **DISCLAIMER**

This document was prepared as an account of work sponsored by the United States Government. While this document is believed to contain correct information, neither the United States Government nor any agency thereof, nor the Regents of the University of California, nor any of their employees, makes any warranty, express or implied, or assumes any legal responsibility for the accuracy, completeness, or usefulness of any information, apparatus, product, or process disclosed, or represents that its use would not infringe privately owned rights. Reference herein to any specific commercial product, process, or service by its trade name, trademark, manufacturer, or otherwise, does not necessarily constitute or imply its endorsement, recommendation, or favoring by the United States Government or any agency thereof, or the Regents of the University of California. The views and opinions of authors expressed herein do not necessarily state or reflect those of the United States Government or any agency thereof or the Regents of the University of California.

Quantitative Aspects of Deuteron (Spin 1) Spin-Decoupling  
in Solids.

D. Suwelack and M. Mehring

Institut für Physik, Universität Dortmund, 46 Dortmund/FRG

and

A. Pines

Dept. of Chemistry, University of Calif., Berkeley, USA

Abstract

The dynamics of heteronuclear spin decoupling in solids is treated rigorously in the case of deuterons ( $^2\text{D}$ ) decoupled from protons ( $^1\text{H}$ ). Dipole-dipole interaction among each spin species is neglected. Deuteron decoupling in the presence of strong quadrupolar interaction  $\omega_Q$  is governed by a double quantum process, which is demonstrated by experiments and by double quantum limit calculations as compared with the rigorous treatment. Double quantum satellites are observed in the proton resonance spectra due to coherent double quantum motion of the deuteron spins.

Work supported by the U. S. Department of Energy.

## I. Introduction

Heteronuclear dipolar coupling  $\chi_{IS}$  between two different spin species I and S is one of the major line broadening mechanism in solids. In fact it is the main line broadening mechanism in diluted spin systems S, where dipolar interaction among the S spins can be neglected<sup>1</sup>. This broadening ranges to about several kHz in solids containing abundant I spins. High resolution S spin magnetic resonance is therefore expected, when the I spins are decoupled by irradiation with strong rf fields at their Larmor frequency  $\omega_{OI}$ .

This aspect of heteronuclear spin decoupling in solids has been of considerable interest in the past. For a review, see reference 2. The influence of the dipolar interaction  $\chi_{II}$  of the abundant I spins on the S spin resonance line has been investigated more recently and interesting aspects of flip-flop spin dynamics have been demonstrated<sup>3</sup>. Especially the "magic angle" quenching of flip-flop terms is clearly displayed<sup>4</sup>. Heteronuclear spin decoupling is heavily applied in recent high resolution nmr techniques applied to solids where high resolution nmr spectra are obtained of either nuclei with low natural abundance (<sup>13</sup>C (1.1 %), <sup>15</sup>N (0.37 %)) or of abundant nuclei, which are homonuclear decoupled by multiple-pulse techniques<sup>2,5</sup>. As an alternative technique for high resolution nmr of protons in solids, the deuteron decoupling of highly deuterated solid samples has been proposed recently<sup>6</sup>. The feasibility of this approach is based on a double quantum transition first observed by Meiboom and co-workers<sup>7</sup>. A review of these techniques can be found in reference 2.

In order to achieve complete decoupling, the field strength  $\omega_{1I} = \gamma_I H_1$  of the decoupling field has to be usually larger than the I spin interactions  $\|\mathcal{H}_I\|$  in the I spin rotating frame, i.e.  $\omega_{1I} \gg \|\mathcal{H}_I\|$ . This condition can be achieved fairly easily if only dipolar interactions are involved. However if  $I > 1/2$  quadrupole interactions of the I spins can be extremely large and single quantum spin decoupling is not feasible. Even in the case of deuterons ( $I=1$ ) the quadrupolar interaction in molecular solids is on the order of 100 kHz, which would require rf fields of several 100 G to decouple the deuterons according to the above requirements.

Since this is technically not feasible, there seemed to be no hope for obtaining high resolution nmr Proton spectra in solids by deuteron decoupling of highly deuterated samples in the past. However, it was Meiboom and co-workers<sup>7</sup> who observed in deuterated liquid crystals, that a double quantum transition allows a much more effective spin decoupling of deuterons than is expected from ordinary single quantum transitions. These findings have been exploited recently in order to obtain high resolution proton spectra in solids by double-quantum decoupling<sup>6,8</sup>. In this publication we want to derive quantitative expressions for the lineshape of deuteron decoupled spectra and we compare exact lineshape calculations with the double quantum limit. Satellite spectra, which display the double quantum coherence are observed for the first time and are explained quantitatively.

## II. Qualitative Aspects of Deuteron Decoupling

For the convenience of the reader let us first repeat the simple arguments about the critical decoupling field strength  $\omega_1^*$  necessary for the onset of decoupling. Suppose two different kind of spins I (with gyromagnetic ratio  $\gamma_I$ ) and S (with gyromagnetic ratio  $\gamma_S$ ) are coupled by dipolar interaction  $\mathcal{H}_{IS}$ . The secular part of the interaction Hamiltonian may then be expressed as

$$\mathcal{H}_{IS} = \sum_{ij} B_{ij} I_{zi} S_{zj} \quad (1)$$

with

$$B_{ij} = -2 \gamma_I \gamma_S \hbar r_{ij}^{-3} P_2(\cos \theta_{ij})$$

where  $r_{ij}$  is the distance between spins i and j and  $\theta_{ij}$  is the angle between the vector  $r_{ij}$  and the magnetic field  $H_0$ . For simplicity we will assume just two spins I and S in the following, although the extension to many spins is straightforward. Later in this section when we come to the general treatment we will relax this restriction and we will treat the many spin case rigorously. Let us discuss two different cases, namely

(i)  $I = 1/2$ ,  $S = 1/2$  where the resonance signal of the S spins will be observed and the I spins will be irradiated with r.f. fields of strength  $\omega_1$ . Without irradiation of the I spins the S spin signal will have a "broadening", which is on the order of the I-S dipolar coupling, i.e.

$$\omega_D = [\text{Tr} \{ \mathcal{H}_{IS}^2 \}]^{1/2} = B/2 \quad (2)$$

When the I spins are irradiated with an r.f. field  $\omega_1$  the following transition rate between  $| -1/2 \rangle$  and  $| +1/2 \rangle$  occurs:

$$W_1 = | \langle 1/2 | \omega_1 I_+ | -1/2 \rangle | = \omega_1 \quad (3)$$

The critical field  $\omega_1^*$  for the onset of decoupling is reached, when

$$\omega_1^* = \omega_D \quad \text{or} \quad \omega_1^* = B/2 \quad (4)$$

i.e. the strength of the r.f. field must be equal to the dipole-dipole interaction in order to break the coupling.

(ii)  $I = 1, S = 1/2$  where the S spin signal will have a "broadening"  $\omega_D$  according to eq. (2) as

$$\omega_D = (2/3)^{1/2} B \quad (5)$$

with no irradiation applied to the I spin resonance. In case the I spins have a strong quadrupole interaction, this leads to a splitting of the I spin resonance into two lines separated by  $2 \omega_Q$  as shown in figure 1. An rf field  $\omega_1$  applied at the center frequency  $\omega_0$  cannot cause transitions from  $| 0 \rangle$  to  $| \pm 1 \rangle$  unless  $\omega_1 \geq \omega_Q$ . Since  $\nu_Q = \omega_Q/2\pi$  may reach values of 100-200 kHz for deuterons in solids r.f. fields of this strength for deuterons are hardly feasible. Although the transition from  $| -1 \rangle$  to  $| +1 \rangle$  vanishes in first order, second order perturbation theory, however, gives the expression<sup>6,7,8</sup>

$$W_2 = (2\omega_1^2/\omega_Q) | \langle 1 | I_x | 0 \rangle \langle 0 | I_x | -1 \rangle | \quad (6)$$



for the transition rate from  $| -1 \rangle$  to  $| +1 \rangle$  corresponding to a double quantum transition.

From Eq. (6) we obtain

$$W_2 = \omega_1 (\omega_1 / \omega_Q) \quad (7)$$

for the double quantum transition rate, i.e.  $\omega_1$  is reduced by the factor  $\omega_1 / \omega_Q$  in the double quantum limit. This very important relation was already utilized in early double quantum decoupling<sup>6-8</sup>. Evaluating the critical field for decoupling as in case (i) we obtain under the condition

$$W_2^* = \omega_D :$$

$$\omega_1^* (\omega_1^* / \omega_Q) = \omega_D \quad \text{or} \quad \omega_1^* = (\omega_D \omega_Q)^{1/2} \quad (8)$$

This equation demonstrates the efficiency of double quantum decoupling, since only the geometric mean of  $\omega_D$  and  $\omega_Q$  is needed for the r.f. field in order to reach the critical field for decoupling<sup>6-8</sup>.

It will be demonstrated in the following, that the double quantum rate  $W_2$  according to equation (7) imposes a coherent motion on the I spins. This motion excites "double quantum satellites" in the S spin spectra, as will be demonstrated in section V.

We shall now turn to some more general and rigorous aspects of spin decoupling with the emphasis on spin I = 1.

### III. Quantitative Aspects of Spin Decoupling

Let us suppose that we observe the resonance signal of dilute S spins (with  $S = 1/2$ ) surrounded by abundant I spins (with  $I \geq 1/2$ ) which will be decoupled by a strong r.f. irradiation

$\omega_1$ , near their Larmor frequency  $\omega_{OI}$ . The free induction decay signal of the S spins after having applied a  $\pi/2$  pulse in the y-direction of the S spin rotating frame may be expressed as

$$G(t) = \text{Tr} \left\{ e^{-it\mathcal{H}} S_x e^{it\mathcal{H}} S_x \right\} / \text{Tr} \left\{ S_x^2 \right\} \quad (9)$$

with

$$\mathcal{H} = \mathcal{H}_{I,I} + \mathcal{H}_I + \mathcal{H}_{I,S}$$

where  $\mathcal{H}$  is the total interaction Hamiltonian in the doubly rotating frame (interaction representation) and  $\text{Tr} \{ \} = \text{Tr}_{I,S} \{ \}$  is the trace operation over I and S variables.

Assuming  $S = 1/2$  and no interaction among the S spins equation (9) may be rewritten after taking the trace over S as

$$G(t) = [(2I+1)^{N_I}]^{-1} \text{Re} \text{Tr}_I \left\{ e^{-it\mathcal{H}(+)} e^{it\mathcal{H}(-)} \right\} \quad (10)$$

where  $N_I$  is the number of the I spins, Re means taking the real part of the trace and  $\mathcal{H}(\pm)$  is the interaction Hamiltonian with  $S_z$  replaced by  $+1/2$  or  $-1/2$  respectively. The free induction decay  $G(t)$  according to equation (10) cannot be calculated rigorously if dipolar interaction among the I spins is involved. This case has been treated approximately using a memory function approach recently<sup>3</sup>. Here we restrict ourselves to the neglect of interactions among the I spins and of course among the S spins. In this case  $[\mathcal{H}_j, \mathcal{H}_k] = 0$  für  $j = k$  an  $G(t)$  can be obtained in product form as

$$G(t) = \text{Re} \prod_j (2I+1)^{-1} \text{Tr}_I \left\{ e^{-it\mathcal{H}_j(+)} e^{it\mathcal{H}_j(-)} \right\} \quad (11)$$

Let us consider some simple examples:

It follows, that

$$\mathcal{H}(\pm) = \omega_1 I_x \pm (B/2) I_z$$

A diagonalization of  $\mathcal{H}(\pm)$  can be obtained by the transformation

$$U(\vartheta) = \exp(i\vartheta I_y)$$

where

$$\sin\vartheta = \omega_1/\Omega ; \cos\vartheta = (B/2)/\Omega$$

with the effective frequency

$$\Omega = [\omega_1^2 + (B/2)^2]^{1/2}$$

Insertion into equation (11) and evaluation of the trace leads to

$$G(t) = \sin^2\vartheta + \cos^2\vartheta \cos\Omega t \quad (12)$$

The limits of

$$\omega_1 = 0; \vartheta = 0; G(t) = \cos(B/2)t \quad (\text{no decoupling})$$

and

$$\omega_1 \gg (B/2); \vartheta = \pi/2; G(t) = 1 \quad (\text{full decoupling})$$

are easily recovered.

In figure 2 we have plotted the amplitude  $R = \cos^2\vartheta$  of the satellite lines at frequency  $\Omega$  as a function of the decoupling field strength  $\omega_1$  in unit of  $B/2$ . Note, that a critical decoupling field  $\omega_1^*$  is reached at the field strength  $B/2$  as obtained also from first order perturbation theory (Eq. 4).  $R$  falls off as  $\omega_1^{-2}$  for  $\omega_1 \gg B/2$ .

The extension to many I spins is straightforward and yields:

$$G(t) = \prod_j [\sin^2\vartheta_j + \cos^2\vartheta_j \cos\Omega_j t] \quad (13)$$

where  $B$  in the above expressions is replaced by  $B_j$ .

Moreover it can be shown, that  $G(t)$  is independent of the phase of the r.f. field in the I rotating frame.

(ii)  $N_I = 1$ ;  $I = 1$ ;  $\chi_{QI} = 0$  (no quadrupole interaction)

The same expressions for  $\chi(\pm)$  and  $U(\nu)$  as in case (i) apply. Evaluating the trace in equation (11) in a similar manner as in case (i) results in

$$G(t) = \frac{1}{3} \left[ 1 + 6 \sin^4 \nu - 4 \sin^2 \nu \right. \\ \left. + 8 \sin^2 \nu \cos^2 \nu \cos \Omega t \right. \\ \left. + 2 \cos^4 \nu \cos 2\Omega t \right] \quad (14)$$

where  $\sin \nu$ ,  $\cos \nu$  and  $\Omega$  are defined as before.

The following spectral lines occur:

	frequency	amplitude
central line	0	$\frac{1}{3} [1 + 6 \sin^4 \nu - 4 \sin^2 \nu]$
satellite	$\pm \Omega$	$\frac{4}{3} [\sin^2 \nu \cos^2 \nu]$
satellite	$\pm 2\Omega$	$\frac{1}{3} \cos^4 \nu$

The limiting case:  $\omega_1 = 0$ ,  $\nu = 0$ ,  $G(t) = [1 + 2 \cos \Omega t] / 3$  (no decoupling) and  $\omega_1 \gg B$ ,  $\nu = \pi/2$ ;  $G(t) \approx 1$  are easily recovered. Let us take the amplitude of the satellite at frequency  $2\Omega$  as a measure of the decoupling efficiency:

$$R = \cos^4 \nu = 1 / [1 + \omega_1^2 / (B/2)^2]^2 \quad (15)$$

This function is plotted versus  $\omega_1$  in figure 2 among other cases to be discussed later. Notice the  $\omega_1^{-4}$  dependence of  $R$  for large  $\omega_1$  in contrast to the  $\omega_1^{-2}$  dependence in the case of  $I = 1/2$  (figure 2).

Again the extension to many I spins is straightforward and can be written as

$$G(t) = \prod_j \frac{1}{3} \left[ 1 + 6 \sin^4 \vartheta_j - 4 \sin^2 \vartheta_j + 8 \sin^2 \vartheta_j \cos^2 \vartheta_j \cos \Omega_j t + 2 \cos^4 \vartheta_j \cos 2\Omega_j t \right] \quad (16)$$

(iii)  $N_I = 1; I = 1; \chi_0 \neq 0$

$$\mathcal{X}(I) = \omega_I I_x + \frac{1}{3} \omega_Q [3I_z^2 - I(I+1)] \pm (B/2) I_z \quad (17)$$

The diagonalization of  $\mathcal{X}(\pm)$  is not as trivial as in the previous cases, although straightforward. Suppose the transformation  $U_1$  diagonalizes  $\mathcal{X}(+)$ , whereas  $U_2$  diagonalizes  $\mathcal{X}(-)$ , resulting in the same diagonal Matrix  $\mathcal{X}_{\text{diag}}$  namely

$$U_1 \mathcal{X}(+) U_1^{-1} = \mathcal{X}_{\text{diag}} = U_2 \mathcal{X}(-) U_2^{-1} \quad (18)$$

with the eigenvalues  $\lambda_1, \lambda_2, \lambda_3$ . The  $\text{Tr}_I \{ \}$  in equation (11) can now be expressed as

$$\begin{aligned} & \text{Re Tr}_I \left\{ \exp(-it \mathcal{X}_{\text{diag}}) U_1 U_2^{-1} \exp(it \mathcal{X}_{\text{diag}}) U_2 U_1^{-1} \right\} \\ &= \sum_{m,k=1,2,3} f_{mk}^2 \cos(\lambda_m - \lambda_k) t \end{aligned} \quad (19)$$

This leads to the free induction decay  $G(t)$  as follows

$$G(t) = \frac{1}{3} \sum_{m,k=1,2,3} f_{mk}^2 \cos(\lambda_m - \lambda_k) t \quad (20)$$

where the expressions for the eigenvalues  $\lambda_j$  of the Hamiltonian

$\chi_{\text{diag}}$  as well as the coefficients  $f_{mk}$  are given in the appendix. The free induction decay can thus be calculated rigorously for arbitrary values of  $\omega_1$  and  $\omega_0$  according to equation (20) in the limit of no dipole-dipole interaction among the deuterons and among the protons.

A typical behavior of the amplitude of the strongest satellite line with  $\omega_1/(B/2)$  as calculated according to eq. (20) is shown in figure 3 for  $\omega_0 = 5 B$  (solid line). Notice that the critical field  $\omega_1^*$  is reached at about 4.5 (B/2), which is considerably less than  $\omega_0$ .

The extension of equation (20) to many I spins is readily obtained as

$$G(t) = \prod_{j=1}^{N_I} \left\{ \frac{1}{3} \sum_{m,k=1,2,3} f_{mk}^2(j) \cos(\lambda_m^{(j)} - \lambda_k^{(j)})t \right\} \quad (21)$$

Summarizing we note, that the analytic expressions of the free induction decay  $G(t)$  in the cases (i) - (iii) are rigorous under the assumption of the neglect of dipolar interaction among the I spins.

In the last case (iii) the diagonalization of the interaction Hamiltonian was performed algebraically and the dynamics involved are easily lost in the procedure. We will therefore attack the problem in a different way by using fictitious spin 1/2 operators in the following<sup>1,9</sup>.

In order to treat double quantum coherence in operator form Vega and Pines<sup>9</sup> introduced fictitious spin 1/2 operators for the spin 1 case recently.

Instead of the Vega-Pines<sup>9</sup> fictitious spin 1/2 operators, however, we prefer here to use the Wokaun-Ernst<sup>10</sup> operators, which refer to the basis of  $I_z$ , i.e.

$$\begin{aligned}
I_x^{r-s} &= \frac{1}{2} \{ |r\rangle\langle s| + |s\rangle\langle r| \} \\
I_y^{r-s} &= -\frac{i}{2} \{ |r\rangle\langle s| - |s\rangle\langle r| \} \\
I_z^{r-s} &= \frac{1}{2} \{ |r\rangle\langle r| - |s\rangle\langle s| \}
\end{aligned} \tag{22}$$

where  $|r\rangle$  and  $|s\rangle$  can take the following values

$$\begin{aligned}
|1\rangle &= | +1 \rangle \\
|2\rangle &= | 0 \rangle \\
|3\rangle &= | -1 \rangle
\end{aligned}$$

as shown in figure 1.

Commutation relations and others among these operators are given in the appendix.

The Hamiltonian  $\mathcal{H}(\pm)$  in equation (17) may now be expressed in terms of these fictitious spin 1/2 operators as<sup>10</sup>

$$\mathcal{H}(\pm) = \pm B I_z^{1-3} + \frac{2}{3} \omega_Q (I_z^{1-2} - I_z^{2-3}) + \sqrt{2} \omega_1 (I_x^{1-2} + I_x^{2-3}) \tag{23}$$

This Hamiltonian  $\mathcal{H}(\pm)$  will now be transformed in different steps, beginning with

$$\mathcal{H}_a = \exp(i\pi/2 I_y^{1-3}) \mathcal{H}(\pm) \exp(-i\pi/2 I_y^{1-3}) \tag{24}$$

After some algebraic manipulation, using the commutation relations and sum rules of the fictitious spin 1/2 operators<sup>10</sup>,

$\mathcal{H}_a$  can be expressed as

$$\mathcal{H}_a = \pm B I_z^{1-3} + 2\omega_1 I_x^{1-2} + \omega_Q I_z^{1-2} + \frac{1}{3} \omega_Q (I_z^{2-3} - I_z^{3-1}) \tag{25}$$

A diagonalization of the  $I^{1-2}$  part can now be achieved by the transformation

$$\mathcal{X}_b = \exp(i\vartheta I_y^{1-2}) \mathcal{X}_a \exp(-i\vartheta I_y^{1-2}) \quad (26)$$

which leads after similar algebraic manipulations as above to<sup>10</sup>

$$\begin{aligned} \mathcal{X}_b = & \pm B \left( I_x^{1-3} \cos \vartheta/2 - I_x^{2-3} \sin \vartheta/2 \right) \\ & + \frac{1}{2} (\omega_e - \omega_0) I_z^{1-3} + \left\{ \frac{2}{3} \omega_0 + \frac{1}{2} (\omega_e - \omega_0) \right\} (I_z^{1-2} - I_z^{2-3}) \end{aligned} \quad (27)$$

where

$$\sin \vartheta = 2\omega_1 / \omega_e ; \cos \vartheta = \omega_0 / \omega_e$$

and

$$\omega_e = [4\omega_1^2 + \omega_0^2]^{1/2} \quad (28)$$

The next step in the transformation procedure is a  $\pi/2$  rotation of the  $I^{1-3}$  part

$$\mathcal{X}_c = \exp(-i\pi/2 I_y^{1-3}) \mathcal{X}_b \exp(i\pi/2 I_y^{1-3}) \quad (29)$$

which leads to

$$\begin{aligned} \mathcal{X}_c = & \pm B I_z^{1-3} \cos \vartheta/2 + \frac{1}{2} (\omega_e - \omega_0) I_x^{1-3} \\ & + \left\{ \frac{2}{3} \omega_0 + \frac{1}{2} (\omega_e - \omega_0) \right\} (I_z^{1-2} - I_z^{2-3}) \\ & \pm (2)^{-1/2} B \sin \vartheta/2 (I_x^{2-3} - I_x^{1-2}) \end{aligned} \quad (30)$$

If we now introduce the assumption  $\omega_1 < \omega_0$  ( $\vartheta \approx 0$ ) in order to neglect  $\sin \vartheta/2$  with respect to  $\cos \vartheta/2$  we reach the



"double quantum limit" and the last term in equation (30) can be neglected, resulting in

$$\mathcal{H}_c^* = \pm B I_z^{1-3} \cos \theta/2 + \frac{1}{2} (\omega_e - \omega_Q) I_x^{1-3} + \left\{ \frac{2}{3} \omega_Q + \frac{1}{2} (\omega_e - \omega_Q) \right\} (I_z^{1-2} - I_z^{2-3}) \quad (31)$$

It is evident, that  $\mathcal{H}_c^*$  can immediately be diagonalized by some transformation  $\exp(i\beta I_y^{1-3})$ , since  $I_y^{1-3}$  commutes with  $(I_z^{1-2} - I_z^{2-3})$ . Before performing this step, however, we would like to discuss equation (31) a little further.

Notice, that  $\mathcal{H}_c^*$  can be separated into two parts

$$\mathcal{H}_c^* = \mathcal{H}_1^{1-3} + \mathcal{H}_2 \quad (32)$$

with

$$[\mathcal{H}_1^{1-3}, \mathcal{H}_2] = 0$$

and where the "double quantum operator"  $\mathcal{H}_1^{1-3}$  introduces transitions between levels 1 and 3.

Since  $\mathcal{H}_1^{1-3}$  commutes with  $\mathcal{H}_2$  we face a similar situation as in the case  $\mathcal{H}_Q = 0$  (cases (i) and (ii)), but now with a double quantum transition involved. The effective r.f. field strength in the double quantum case, however, is reduced by a scaling factor  $\omega_1/\omega_Q$  as follows from (eq. 31)

$$\frac{1}{2} (\omega_e - \omega_Q) \approx \omega_1^2 / \omega_Q \quad \text{when } \omega_1 \ll \omega_Q$$

Note, that the same result was obtained from second order perturbation theory<sup>6,7</sup> (Eq. 7), demonstrating the role of the r.f. field  $\omega_1^2/\omega_Q$  in the double quantum frame<sup>9</sup>.

Experimental consequences of this will be shown in section V.

Under the assumption  $\omega_1 \ll \omega_Q$  the transformed Hamiltonian

$\mathcal{H}_c^*$  in the double quantum limit may now be rewritten as

$$\mathcal{H}_c^* \approx \pm B I_z^{1-3} + (\omega_1^2/\omega_0) I_x^{1-3} + \frac{2}{3} \omega_0 (I_z^{1-2} - I_z^{2-3}) \quad (33)$$

This is virtually the same Hamiltonian as  $\mathcal{H}(\pm)$  in equation (23) where  $\sqrt{2} \omega_1 (I_x^{1-2} + I_x^{2-3})$  has been replaced by  $(\omega_1^2/\omega_0) I_x^{1-3}$  and where the 1-3 part commutes with  $(I_z^{1-2} - I_z^{2-3})$ . In this limit spin dynamics introduced by the r.f. field is restricted to the double quantum frame and can be treated in a simple fashion as was done in the cases (i) and (ii) ( $\mathcal{H}_0 = 0$ ).

We now come back to the more general expression of  $\mathcal{H}_c^*$  as given by equation (31) and perform the transformation

$$\mathcal{H}_d^* = \exp(\pm \beta I_y^{1-3}) \mathcal{H}_c^* \exp(\mp i \beta I_y^{1-3}) \quad (34)$$

which leads to

$$\mathcal{H}_d^* = \pm \Omega I_z^{1-3} + \left\{ \frac{2}{3} \omega_0 + \frac{1}{2} (\omega_e - \omega_0) \right\} (I_z^{1-2} - I_z^{2-3}) \quad (35)$$

where

$$\sin \beta = \left[ \frac{1}{2} (\omega_e - \omega_0) \right] / \Omega^*; \quad \cos \beta = B \cos(\vartheta/2) / \Omega^* \quad (36a)$$

and

$$\Omega^* = \left\{ (B \cos \vartheta/2)^2 + \left[ \frac{1}{2} (\omega_e - \omega_0) \right]^2 \right\}^{1/2} \quad (36b)$$

In the limit  $\omega_1 \ll \omega_0$  this again reduces to

$$\sin \beta = \omega_1^2 / (\omega_0 \Omega^*); \quad \cos \beta = B / \Omega^* \quad (37a)$$

with 
$$\Omega^* = \left[ B^2 + (\omega_1^2/\omega_0)^2 \right]^{1/2} \quad (37b)$$

The Hamiltonian  $\mathcal{H}_d^*$  is in diagonal form and can be readily used to calculate the trace in equation (11) and thus the free induction decay. The total transformation used may be

summarized as

$$U_{\text{total}} = U(\pm\beta) U(\nu) \quad (38)$$

where

$$U(\nu) = \exp(-i\nu/2 I_y^{1-3}) \exp(i\nu I_y^{1-2}) \exp(i\nu/2 I_y^{1-3}) \quad (39)$$

and

$$U(\pm\beta) = \exp(\pm i\beta I_y^{1-3}) \quad (40)$$

Evaluation of the trace in equation (11) by using the transformation  $U_{\text{total}}$  (Eq. 38) and the diagonal Hamiltonian  $\mathcal{H}_d^*$  (Eq. (35)) proceeds along the same lines as in case (ii) and results in

$$G(t) = \frac{1}{3} [1 + 2 \sin^2\beta + 2 \cos^2\beta \cos \Omega^* t] \quad (41)$$

where  $\sin\beta$ ,  $\cos\beta$  and  $\Omega^*$  are given by Eq. (36) in the limit  $\omega_1 < \omega_0$  and by Eq. (37) in the limit  $\omega_1 \ll \omega_0$ .

A central line with intensity  $(1+2 \sin^2\beta)/3$  is observed together with two satellite lines at the frequency  $\pm \Omega^*$  with intensity  $\cos^2\beta$ . It is instructive to compare this double quantum limit with the case (ii) ( $\mathcal{X}_0 = 0$ ) and the rigorous calculation in case (iii) ( $\mathcal{X}_0 \neq 0$ ).

Especially the question arises: Is the double-quantum limit (Eq. 41) a good enough approximation to the rigorous result (Eq. 20) in practical cases. In figure 4 we have plotted spectral lines for the two different cases with the quadrupole interaction  $\omega_0 = 2B$  for different parameters  $\omega_1/(B/2)$ . Notice, that only a slight difference is observed in the spectra derived from the rigorous (exact) and the double quantum limit calculation respectively. We have also calculated

lineshapes for many-spin interactions for different configurations of deuterons. In all these cases there is only a minute difference between the exact lineshape according to (Eq. 20) and the double quantum limit (Eq. 41). Further we would like to note, that the behavior of the critical decoupling field  $\omega_1^* \sim [\omega_Q \omega_D]^{1/2}$  is also displayed in figure 4. Similar spectra have been obtained by Emsley et al.<sup>11</sup> by means of computer diagonalization.

The amplitude variation of the strongest satellite lines are compared for the rigorous (Eq. 20) and the double quantum limit (Eq. 41) calculations with  $\omega_Q = 5 B$  in figure 3. The overall behavior is quite similar for both calculations. Notice, that the critical field  $\omega_1^* = 4.5(B/2)$  is close to the value expected from second order perturbation theory, namely (Eq. 5, 8)

$$\omega_1^* = [\omega_Q \cdot \omega_D]^{1/2} = 4.04 (B/2)$$

The deviation of the double quantum limit calculation from the rigorous treatment decreases drastically for larger quadrupolar interaction  $\omega_Q$ .

The extension to many I spins with no interaction among each other is again straightforward and is as given here for completeness

$$G(t) = \prod_j \frac{1}{3} [1 + 2 \sin^2 \beta_j + 2 \cos^2 \beta_j \cos \Omega_j^* t] \quad (42)$$

where B and  $\omega_Q$  in the above expressions have to be replaced by  $B_j$  and  $\omega_{Qj}$  respectively. Free induction decays and spectra have been calculated according to equation (42) and are compared with experimental data in section V.

#### IV. Experimental

Experiments were performed on highly deuterated ( $\geq 98\%$ ) hexamethylbenzene (HMB) and squaric acid (SQA) with different grades of deuteration. Single crystals were grown from aqueous solutions. The applied magnetic field was 6.3 Tesla, which corresponds to the resonance frequency of 270 MHz for the observed proton signal and to 46.45 MHz for the decoupled deuterons.

The r.f. fields at both frequencies were applied to the sample in a homebuilt single coil double resonance probehead. The 270 MHz channel was equipped with a Bruker pulse spectrometer SXP 4-100/270, whereas the decoupling channel (46.45 MHz) employed a homebuilt double resonance spectrometer. At the deuteron frequency r.f. fields up to 100 G could be obtained. Data accumulation and storage was performed in a homebuilt averager and Fourier transformed by a Varian 620 L computer. All measurements were performed at roomtemperature.

#### V. Results and Discussion

A representative example of the proton lineshape in highly deuterated hexamethylbenzene (HMB) is shown in figure 5 for a decoupling field strength of  $\omega_1 = 2\pi \cdot 3.2$  kHz and a quadrupole interaction of  $\omega_Q = 2\pi \cdot 8.0$  kHz. HMB has the interesting property, that all deuterons in the unit cell are magnetically equivalent due to rapid molecular reorientation, i.e. only a single value of the quadrupole interaction  $\omega_Q$  is observed, depending on the angle  $\beta$  of the molecular sixfold axis with respect to the magnetic field as

where  $\omega_{Q0} = 2\pi \cdot 16$  kHz in HMB.

The theoretical lineshape was calculated using the given molecular and crystal structure together with the measured value for the quadrupole interaction  $\omega_Q$ . No detectable difference between the exact (Eq. 21) and the double quantum limit (Eq. 42) calculation was observed.

In figure 5 we compare the calculated and the experimental lineshape and find a fairly good agreement. Notice, the satellite peaks in figure 5, which are due to the coherent spin motion caused by the double quantum transition with a rate of about  $\omega_1^2/\omega_Q$ . The satellite frequency  $\nu_s$  as obtained from similar spectra for different values of  $\omega_1$  is plotted versus  $\omega_1$  in figure 6. The theoretical curve (solid line) in figure 6 derives from calculated lineshapes as shown in figure 5. The agreement with the experimental data is quite pleasing. Also the rough estimate of the satellite frequency  $\nu_s$  by  $\omega_1^2/\omega_Q$  (dashed line) shows the correct trend.

In order to investigate the decoupling efficiency we have measured the linewidth of the proton resonance line in HMB for different decoupling fields  $\omega_1$ . Typical results for two different  $\omega_Q$  values are plotted in figure 7, together with the theoretically determined normalized linewidth  $\delta_r$ . The calculations were done rigorously (Eq. (21)) as well as in the double quantum limit (Eq. (42)) with no noticeable difference in figure 7. Notice also the rapid decrease of the linewidth once the critical field  $\omega_1^*$  is reached. This behavior was also demonstrated in the coherent average approach as used previously<sup>6</sup>. From the simple formula (Eq. (8)) the critical field should be proportional to  $(\omega_Q \omega_D)^{1/2}$ . We have therefore plotted

$\omega_1^*$  versus  $[\omega_Q \omega_D]^{1/2}$  in figure 8. Different values of  $\omega_Q$  and  $\omega_D$  were obtained by different orientations of the HMB crystal in the magnetic field. The critical field  $\omega_1^*$  was obtained from plots like figure 7. The calculated curve (solid line) follows from rigorous as well as double quantum limit calculations and represents the data quite accurately. The simple expression  $\omega_1^* = (\omega_Q \omega_D)^{1/2}$  (dashed line) obtained from second order perturbation theory does show the general trend, but deviates from the experimental data appreciably.

Finally we want to demonstrate again, that this technique might be usefull for obtaining high resolution proton nmr spectra in solids, by showing the deuteron decoupled proton spectrum in highly deuterated squaric acid ( $C_4O_4H_2$ ), where the proton chamental shift tensor has been determined previously<sup>12</sup> (see figure 9). The residual proton linewidth was investigated for different grades of dilution in this compound. An account on this will be reported later.

## VI. Conclusion

Proton line broadening of diluted protons immersed in a deuterated matrix can be calculated quantitatively for arbitrary strength of the decoupling field  $\omega_1$ . The spin dynamical process involved is a double quantum transition, which makes the decoupling very efficient. Lineshape calculations show that only minute differences occur for rigorous and double quantum limit calculations. Coherent spin motion due to the double quantum transitions is observed as "double quantum satellites" in the proton spectra. All these phenomena can be accounted for quantitatively.

VII. Acknowledgements: The single crystal of HMB was kindly grown by H.Zimmermann. Intensive discussions with Dr. S. Vega on double quantum decoupling is gratefully acknowledged. The Deutsche Forschungsgemeinschaft has given considerable financial support.



## VIII. Appendix

(a) Diagonalization of  $\mathcal{X}(\pm)$ 

$$\mathcal{X}(\pm) = \omega_1 I_x + \frac{1}{3} \omega_Q [3I_z^2 - I(I+1)] \pm (B/2) I_z \quad (\text{A1})$$

Diagonalization of  $\mathcal{X}(\pm)$  is achieved by the transformation

$$U_1 \mathcal{X}(\pm) U_1^{-1} = \mathcal{X}_{\text{diag.}} = U_2 \mathcal{X}(\pm) U_2^{-1} \quad (\text{A2})$$

where

$$U_1 = \begin{pmatrix} r_{11} & r_{12} & r_{13} \\ r_{21} & r_{22} & r_{23} \\ r_{31} & r_{32} & r_{33} \end{pmatrix}; \quad U_2 = \begin{pmatrix} -r_{13} & -r_{12} & -r_{11} \\ r_{23} & r_{22} & r_{21} \\ r_{33} & r_{32} & r_{31} \end{pmatrix} \quad (\text{A3})$$

with

$$r_{il} = r'_{il} / \left( \sum_{k=1}^3 r'_{ik}{}^2 \right)^{1/2} \quad i, l = 1, 2, 3 \quad (\text{A4})$$

and

$$r'_{11} = \lambda_2 \lambda_3 - (\lambda_2 + \lambda_3) Q_- + Q_-^2 + \omega_1^2 / 2$$

$$r'_{12} = -\omega_1 (\lambda_2 + \lambda_3 + Q_+) / \sqrt{2} \quad (\text{A5})$$

$$r'_{13} = \omega_1^2 / 2$$

$$r'_{21} = -\omega_1 (\lambda_1 + \lambda_3 + Q_+) / \sqrt{2}$$

$$r'_{22} = \lambda_1 \lambda_2 + \frac{2}{3} \omega_Q (\lambda_1 + \lambda_3) + \omega_1^2 + \frac{4}{9} \omega_Q^2$$

$$r'_{23} = -\omega_1 (\lambda_1 + \lambda_3 + Q_-) / \sqrt{2}$$

$$r'_{31} = \omega_1^2 / 2$$

$$r'_{32} = -\omega_1 (\lambda_1 + \lambda_2 + Q_-) / \sqrt{2}$$

The eigenvalues  $\lambda_1, \lambda_2, \lambda_3$  of  $\chi_{\text{diag}}$  are then given by

$$\begin{aligned}\lambda_1 &= -2p \cos(\varphi/3 + 60^\circ) \\ \lambda_2 &= -2p \cos(\varphi/3 - 60^\circ) \\ \lambda_3 &= 2p \cos(\varphi/3)\end{aligned}\tag{A6}$$

with

$$\cos \varphi = -q/p^3\tag{A7}$$

$$p = \left[ (\omega_{a/3})^2 + (B/2)^2/3 + \omega_1^2/3 \right]^{1/2}\tag{A8}$$

$$q = (\omega_{a/3}) \left[ (\omega_{a/3})^2 - (B/2)^2 + \omega_1^2/2 \right]\tag{A9}$$

From equation (19),  $G(t)$  follows readily as

$$G(t) = \frac{1}{3} \sum_{m,k=1,2,3} f_{mk}^2 \cos(\lambda_m - \lambda_k)t\tag{A10}$$

where  $\lambda_1, \lambda_2, \lambda_3$  are given by Eqs. (A6) - (A9) and with

$$F = \{f_{mk}\} = U_2 U_1^{-1}\tag{A11}$$

(b) Fictitious spin 1/2 operators for  $I = 1$  in the Wokaun-Ernst notation<sup>10</sup>.

$$\begin{aligned}I_x^{r-s} &= \frac{1}{2} \{ |r\rangle\langle s| + |s\rangle\langle r| \} \\ I_y^{r-s} &= \frac{-i}{2} \{ |r\rangle\langle s| - |s\rangle\langle r| \} \\ I_z^{r-s} &= \frac{1}{2} \{ |r\rangle\langle r| - |s\rangle\langle s| \}\end{aligned}\tag{A12}$$

with

$$\bar{I}_x^{s-r} = \bar{I}_x^{r-s}; \quad \bar{I}_y^{s-r} = -\bar{I}_y^{r-s}; \quad \bar{I}_z^{s-r} = -\bar{I}_z^{r-s} \quad (\text{A13})$$

For the convenience of the reader, we summarize some of the relations of the operators  $\bar{I}_\alpha^{r-s}$ ,  $\alpha = x, y, z$  following Wökaun-Ernst<sup>10</sup> (for  $I = 1$ ):

$$\bar{I}_{x|y} = \sqrt{2} (\bar{I}_{x|y}^{1-2} + \bar{I}_{x|y}^{2-3}) \quad (\text{A14})$$

$$\bar{I}_z = 2 (\bar{I}_z^{1-2} + \bar{I}_z^{2-3}) \quad (\text{A15})$$

and with

$$\bar{I}_z^{1-2} + \bar{I}_z^{2-3} + \bar{I}_z^{3-1} \quad (\text{A16})$$

follows

$$\bar{I}_z = \bar{I}_z^{1-2} + \bar{I}_z^{2-3} + \bar{I}_z^{3-1} = 2\bar{I}_z^{1-3} \quad (\text{A17})$$

The following commutation rules apply:

$$[\bar{I}_\alpha^{r-s}, \bar{I}_\beta^{r-s}] = i \bar{I}_\gamma^{r-s} \quad \alpha, \beta, \gamma = x, y, z \quad (\text{A18})$$

(cyclic)

and

$$\begin{aligned} [\bar{I}_x^{r-t}, \bar{I}_x^{s-t}] &= [\bar{I}_y^{r-t}, \bar{I}_y^{s-t}] = (i/2) \bar{I}_y^{r-s} \\ [\bar{I}_x^{r-t}, \bar{I}_y^{s-t}] &= (i/2) \bar{I}_x^{r-s} \\ [\bar{I}_x^{r-t}, \bar{I}_z^{s-t}] &= (-i/2) \bar{I}_y^{r-t} \\ [\bar{I}_y^{r-t}, \bar{I}_z^{s-t}] &= (i/2) \bar{I}_x^{r-t} \\ [\bar{I}_z^{r-t}, \bar{I}_z^{s-t}] &= 0 \end{aligned} \quad (\text{A19})$$

where  $r, s, t$  are all unequal.

References

1. A.Abragam, Principles of Nuclear Magnetism,  
Oxford Univ.Press, London 1961
2. M.Mehring, High Resolution NMR Spectroscopy in Solids,  
NMR: Basic Principles and Progress, Vol.11,  
Springer 1976
3. M.Mehring and G. Sinning, Phys. Rev. B15, 2519 (1977)
4. M.Mehring, G.Sinning and A.Pines, Z.Phys. B24, 73 (1976)
5. U.Haeberlen, Advances in Magn. Res. (supplement)  
Academic Press, New York 1976
6. A.Pines, D.J.Ruben, S.Vega and M.Mehring, Phys.Rev.Lett. 36, 110  
(1976)
7. R.C.Hewitt, S.Meiboom, L.C.Snyder, J.Chem.Phys. 58, 5089 (1973)  
L.C.Snyder and S.Meiboom, J.Chem.Phys. 58, 5096 (1973)
8. A.Pines, S.Vega and M.Mehring, Phys.Rev. (in press)
9. S.Vega and A.Pines, J.Chem.Phys. 66, 5624 (1977)
10. A.Wokaun and R.R.Ernst, J.Chem.Phys. 67, 1752 (1977)
11. J.W.Emsley, J.C.Lindon and J.M.Tabong, J.Chem. Soc.,  
Faraday Trans. II 69, 10 (1973)
12. D.Suwelack, J.D.Becker and M.Mehring, Sol.State Comm.  
22, 597 (1977)

Figure Captions

Fig. 1 Energy level diagram of a spin 1 in a magnetic field  $H_0$  including quadrupolar interaction  $\omega_Q$ . Two satellite lines at  $\omega_0 \pm \omega_Q$  are observed as single quantum transitions ( $\Delta m = 1$ ). The double quantum transition ( $\Delta m = 2$ ) at  $2\omega_0$  is indicated.

Fig. 2 Amplitude R of the satellite transition for a spin  $I = 1/2$  (single quantum transition) (Eq.(12)) versus decoupling field strength  $\omega_1$  in units of the dipolar interaction  $B/2$ . A "critical" field is reached at  $\omega_1^* = B/2$ .

Fig. 3 Amplitude R of the strongest satellite transition for a spin  $I = 1/2$  with and without quadrupolar interaction  $\omega_Q$  versus decoupling field strength  $\omega_1$ . In the case  $\omega_Q = 0$  R is given by Eq. (15) (dotted curve), whereas for  $\omega_Q \neq 0$  a rigorous (Eq. (41), dashed curve), as well as a double quantum limit calculation (Eq. (41), dashed curve) are compared. A critical field of  $\omega_1^* \approx 4.5 (B/2)$  is reached in the case  $\omega_Q = 5 B$ .

Fig. 4 Spectral lines of a spin  $S = 1/2$  coupled to a spin  $I = 1$  by dipolar interaction  $B$  for different values of the decoupling field strength  $\omega_1$  applied at the Larmor frequency of the I spins. The quadrupole interaction of the I spins is fixed at  $\omega_Q = 2B$ . Rigorous (solid line) calculations

according to Eq. (20) are compared with double quantum limit (dashed lines) calculations according to Eq. (41). For larger  $\omega_0$  values both calculations are hardly distinguishable.

Fig. 5

Proton resonance spectra (dotted curve) at 270 MHz of highly deuterated (98 %) hexamethylbenzene (HMB) for  $\nu_0 = 8.0$  kHz and  $\nu_1 = 3.2$  kHz. The theoretical lineshape (solid curve) was calculated according to Eq. (21) (rigorous) as well as Eq. (42) (double quantum limit) by using the molecular and crystal structure data together with the values for  $\omega_0$  and  $\omega_1$  as given above. Notice the "double quantum satellites" at about  $\nu_1^2/\nu_0$ .

Fig. 6

Double quantum satellite frequency  $\nu_s$  as obtained from spectra like figure 5 versus decoupling field  $\omega_1$ . The theoretical curve (solid line) derives from lineshape calculations like in figure 5, whereas the dashed line represents the simple relation  $\nu_s = \nu_1^2/\nu_0$ .

Fig. 7

Normalized line width  $\delta_n$  of proton spectra in deuterated HMB versus decoupling field  $\omega_1$  for different values of the quadrupole interaction  $\omega_Q$  of the deuterons. The theoretical curves (solid lines) are obtained by taking the linewidth of spectra, which were calculated rigorously (Eq. (21)) as well as in the double quantum limit (Eq. (42)), with both calculations leading to indistinguishable

results on the scale of the drawing.

Fig. 8 Critical decoupling field  $\omega_1^*$  ( $\delta_n = 1/2$ ) as obtained from data like those presented in figure 7 versus  $(\omega_0 \omega_D)^{1/2}$ . The theoretical line (solid lines) derives from critical fields  $\omega_1^*$  at  $\delta_n = 1/2$  as obtained from similar theoretical curves as in figure 7.

Fig. 9 High resolution proton spectra at 270 MHz in highly deuterated (99 %) squaric acid by deuteron decoupling.

$\omega_0 = 0$        $\omega_0 \neq 0; \omega_a = 0$        $\omega_0 \gg \omega_a \neq 0$

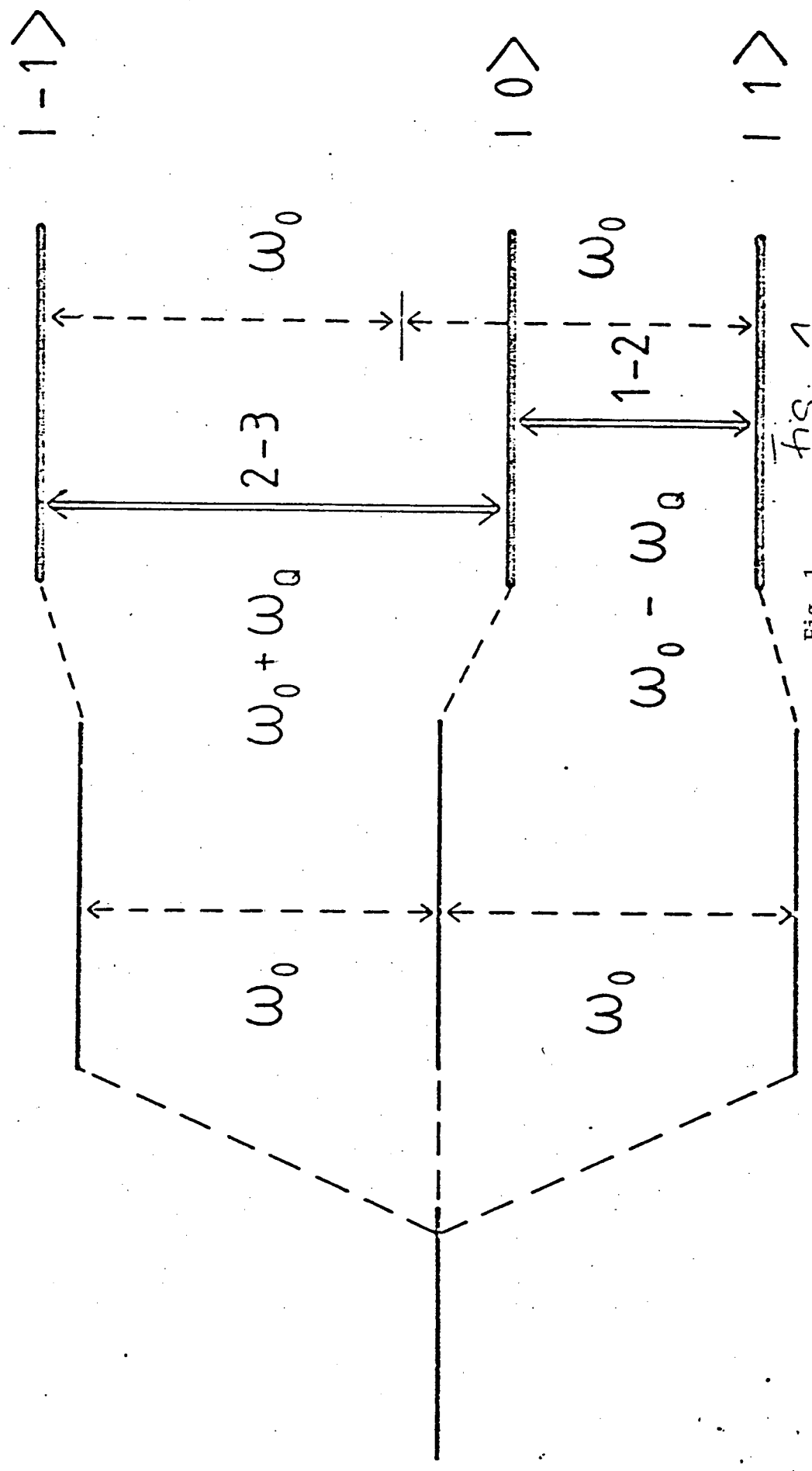


Fig. 1



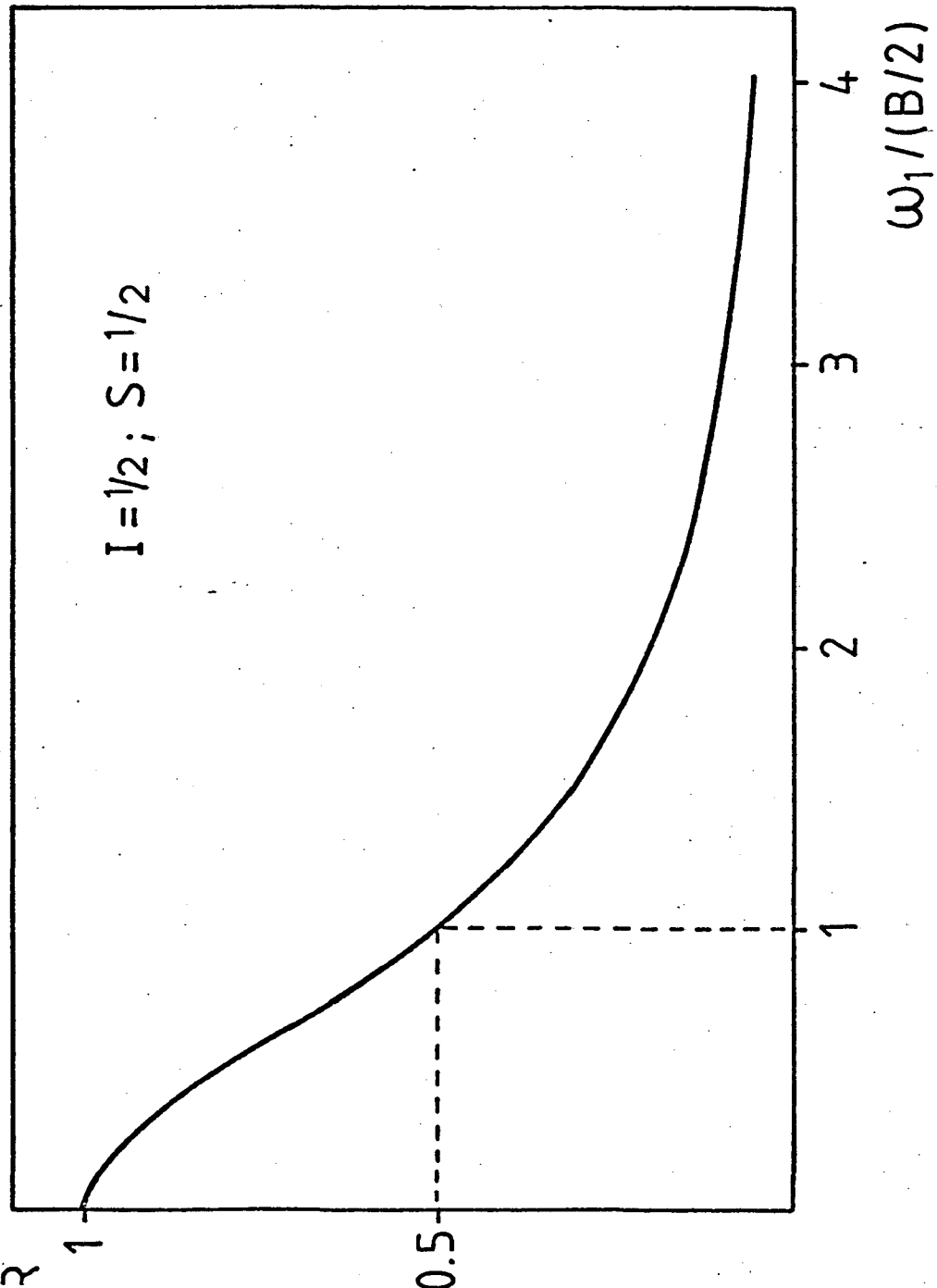


Fig. 2

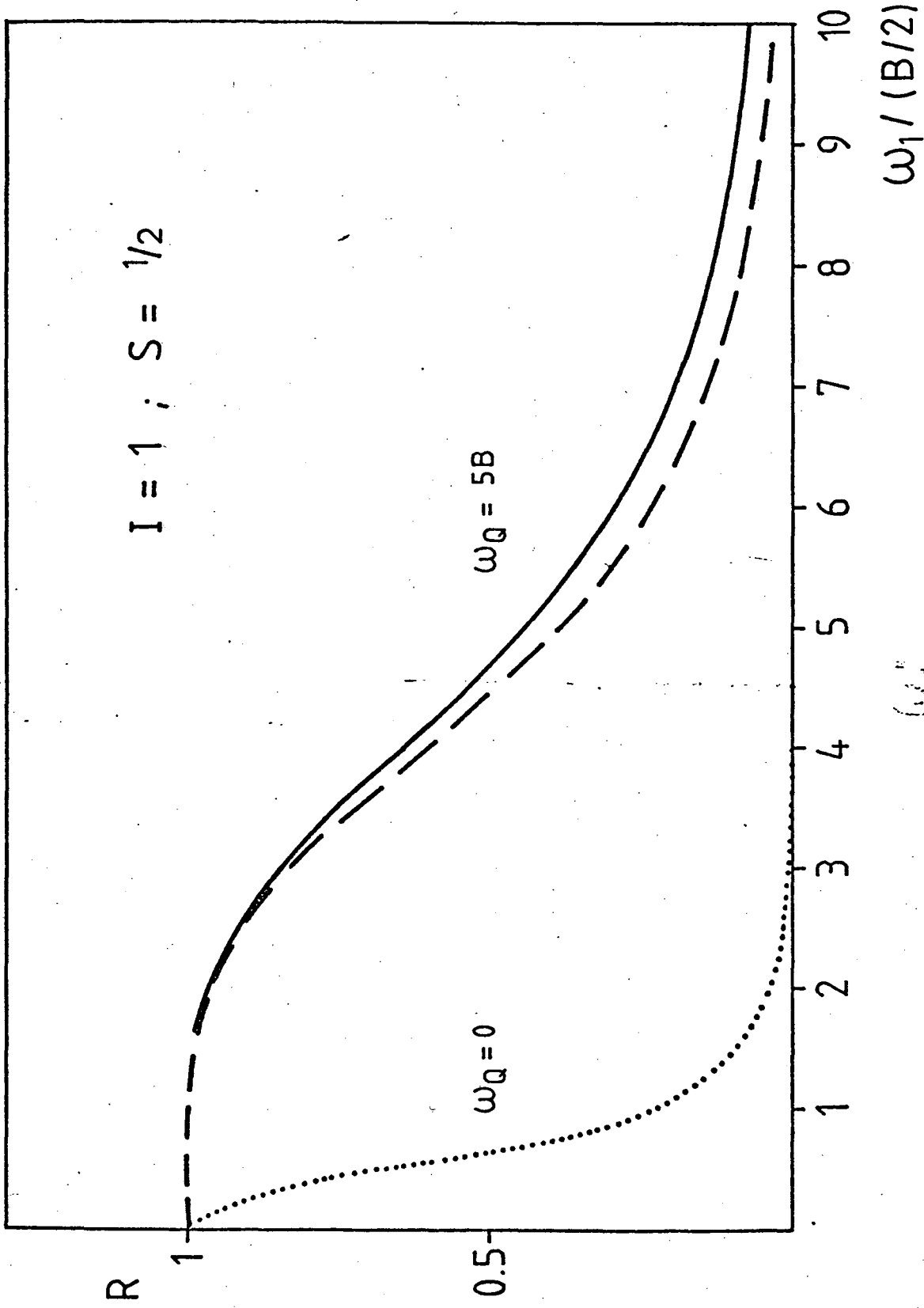
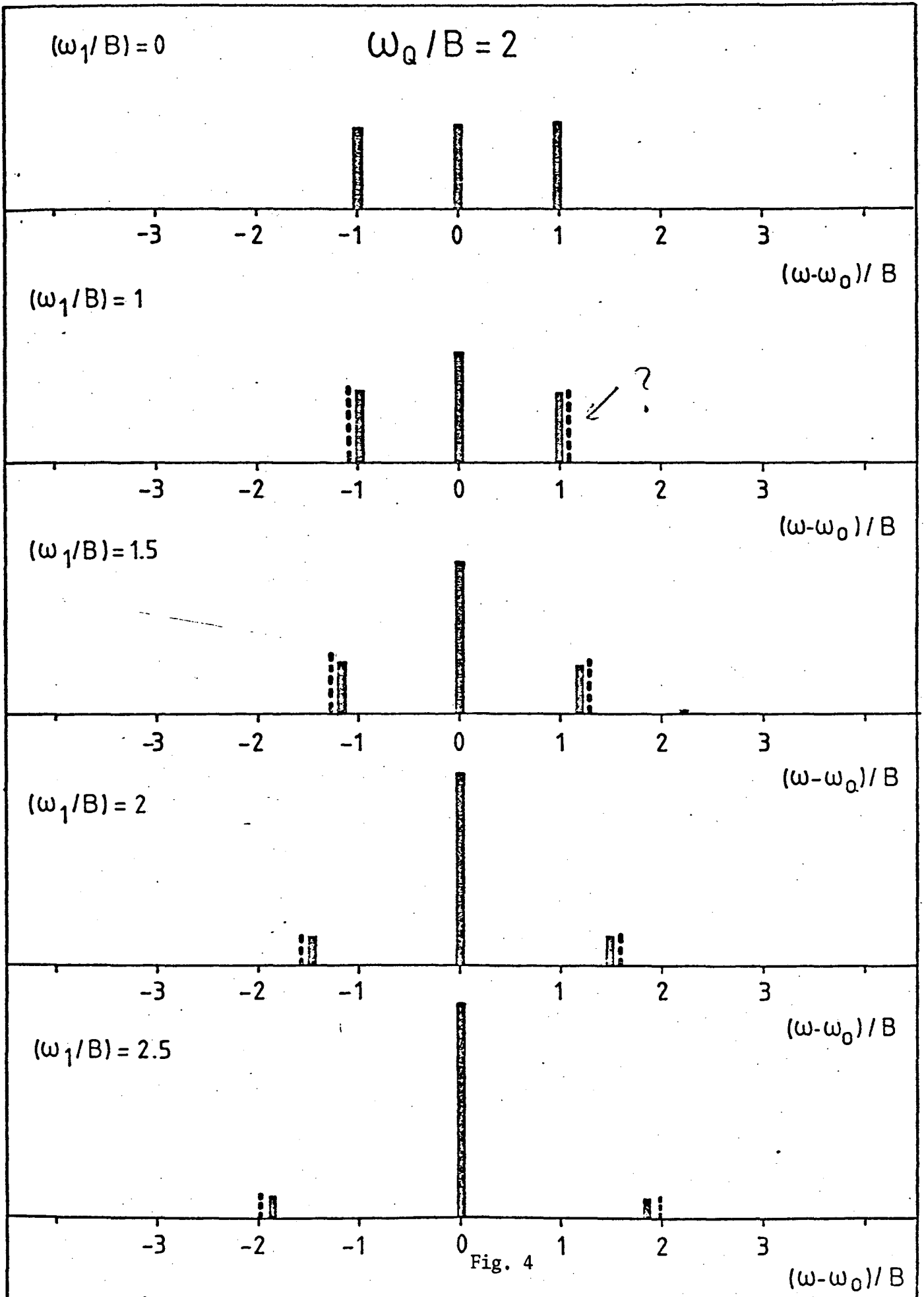


Fig. 3



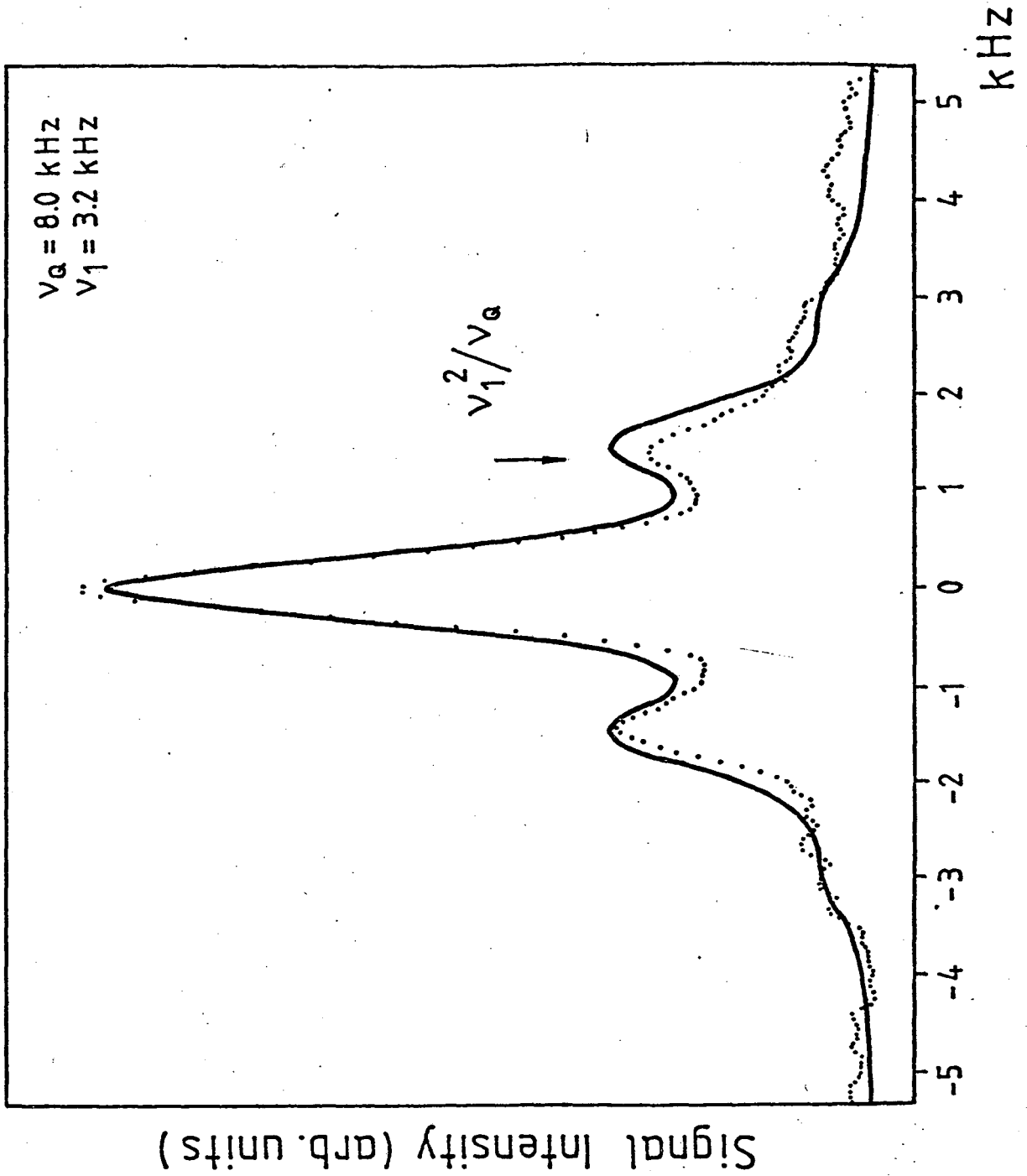


Fig. 5

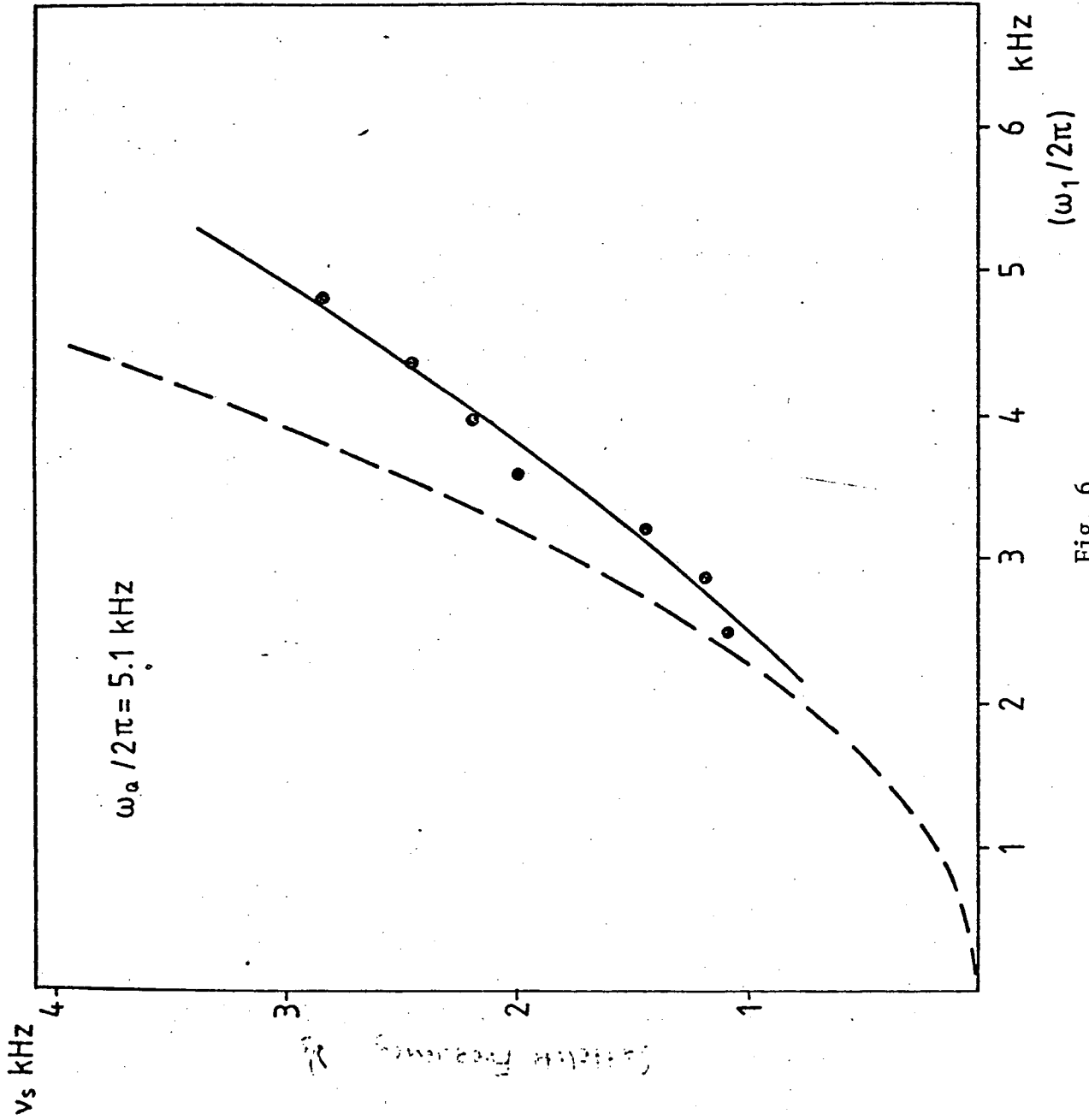


Fig. 6

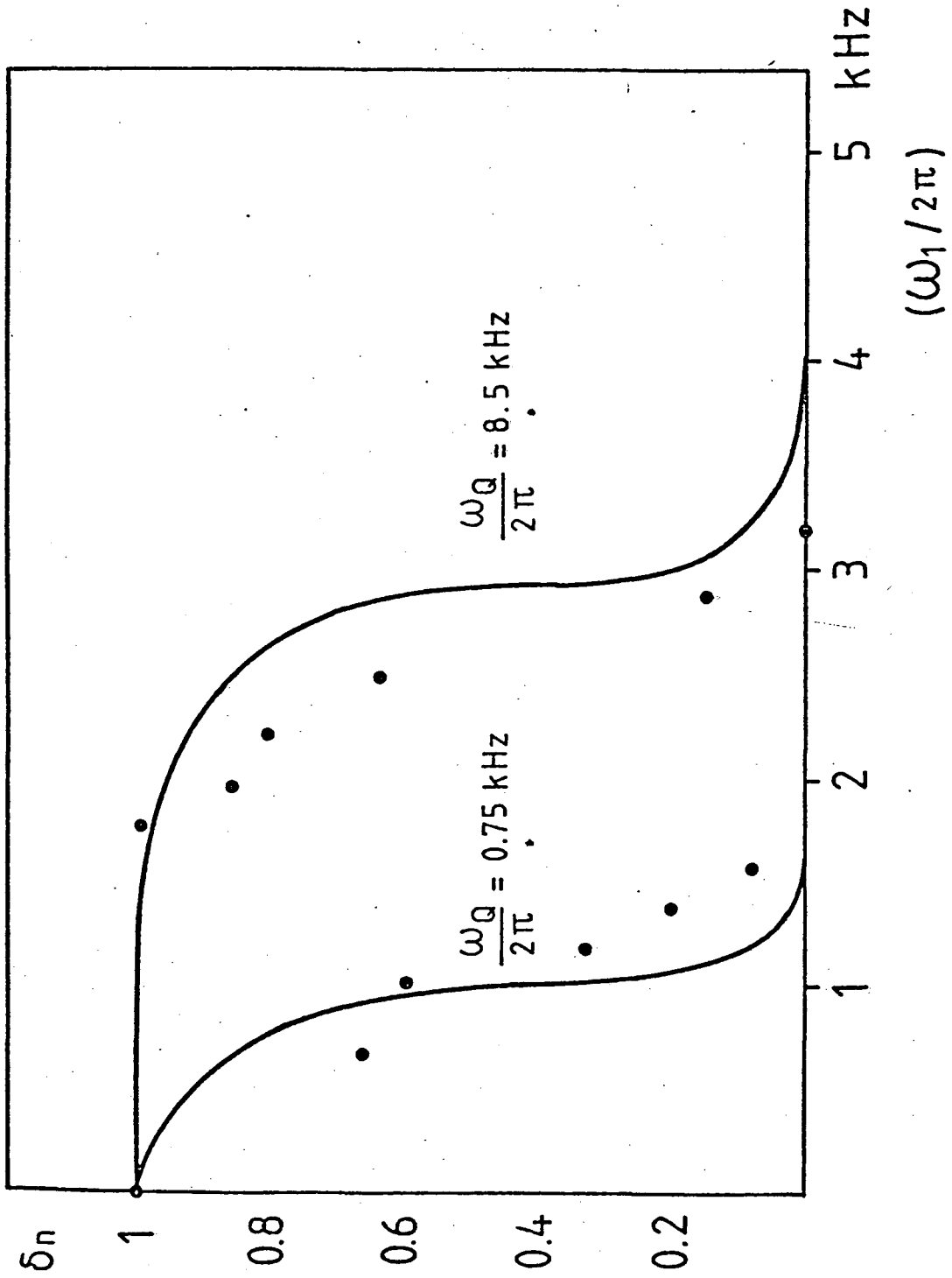


Fig. 7

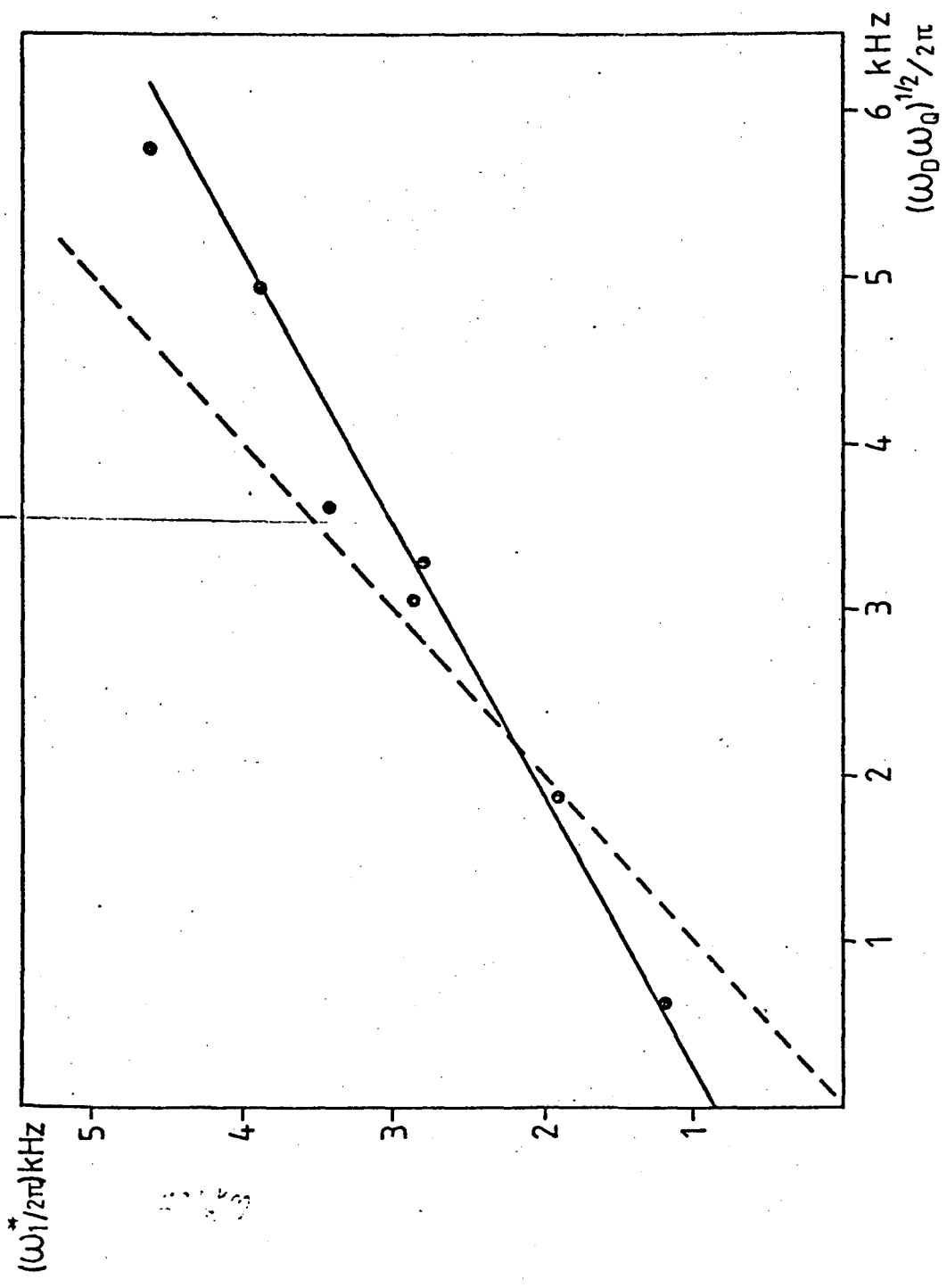


Fig. 8



This report was done with support from the Department of Energy. Any conclusions or opinions expressed in this report represent solely those of the author(s) and not necessarily those of The Regents of the University of California, the Lawrence Berkeley Laboratory or the Department of Energy.



TECHNICAL INFORMATION DEPARTMENT  
LAWRENCE BERKELEY LABORATORY  
UNIVERSITY OF CALIFORNIA  
BERKELEY, CALIFORNIA 94720